Scale-model ridges and interaction with narrow structures, Part 1 Overview and scaling

Aleksey Shestov[1], Aase Ervik[2], Jaakko Heinonen[3], Ilka Perälä[3], Knut V. Høyland[1,4], Evgenii Salganik[4], Hongtao Li[4], Marnix van den Berg[4], Zongyu Jiang[4] and Otto Puolakka[5]

1 The University Centre in Svalbard (UNIS), Norway
2 Multiconsult AS, Norway
3 Technical Research Centre of Finland (VTT), Finland
4 The Norwegian University of Science and Technology (NTNU), Norway
5 Aalto University, Finland
Aleksey.shestov@unis.no, knut.hoyland@ntnu.no, Evgenii.salganik@ntnu.no

Abstract

An experimental campaign to investigate sea ice ridge interaction with bottom-fixed structures was carried out in the Aalto ice basin. Ice ridges were produced, their consolidation was monitored, the properties of level ice and ridges were tested. Finally, a structure was pulled through the level ice and ridges while measuring the loads and monitoring the deformation pattern. Two different structures were tested, one with cylindrical and one with a conical waterline shape. We investigated a) the scaled ridge properties, b) how structures broke level ice and ice ridge, and c) the scaling of ridge forces with respect to a cylindrical and a conical structure at the waterline. Full-scale ridge structure interaction data are available for the Norströmsgrund lighthouse, so we used its size in scaling the tests. We assumed that gravity/buoyancy forces contribute and combined Froude and Strength scaling with a geometric scale-factor of 15. The initial ice temperature and accumulated air temperatures (FDD) during consolidation were varied to investigate how reasonably scaled ridge properties can be achieved. The campaign covered three different ice sheets and ridges. Punch tests, flexural strength, compressive strength tests were carried out. The main preliminary observations are that loads from level ice on vertical structure (F^V_{li}) gave the highest load. Next, in decreasing order of magnitude, followed the load from a ridge on vertical structure (F^V_{ri}), load from a ridge on sloping structure (F^S_{ri}), and finally, the load from level ice on sloping structure (F^S_{li}).

1. Introduction

Ice ridges are often key features when designing structures in ice-covered waters. In the case of only first-year ice and that icebergs do not exist or can be managed, first-year ice ridges give the quasi-static design load. In the Baltic, there are plans to expand electricity production from Offshore wind, and one of the essential questions concerning structure design is if a cylindrical or conical structure shape at the waterline should be used. A conical structure reduces the ice load as long as it provokes bending failure instead of crushing. However, there are several disadvantages. It is more expensive to produce. It gives higher hydrodynamic loads than the cylindrical structure. It makes ship access (for maintenance) more difficult, and the cone may become very large in waters with a high tidal difference. To estimate ridge loads, ISO19906 (2019) gives models for the ice rubble and recommends using level ice formulas for the consolidated layer. There are several problems with this. The formula for ice rubble action does not include surcharge even though it is included in the original paper (Dolgopolov et al., 1975), and Serré and Liferov (2010) argue that this is important. Further, the level ice action on sloping structures includes the effects of ice rubble accumulation. However, in a ridge, there are already large amounts of rubble. We think that the level ice interaction with accumulating rubble is not directly transferable to how the consolidated layer produces accumulating rubble and interacts with it. Finally, the effect of steep cones is not apparent even for level ice. It has not been shown which cone angles ensure bending failure.

Experiments in the Aalto ice basin were planned and conducted with ridge action on fixed vertical and steep-cone structures. There were two somewhat different, but connected topics:
a) The production and scaling of ice ridges in model-scale
b) The effect of the steep cone on the total load from ridges and surrounding level ice

The Norströmsgrund lighthouse offshore Luleå was instrumented in the LOLEIF and STRICE project and is still the best dataset for full-scale ice interaction with vertical structures. We will use a scaled version of this lighthouse as the vertical model-scale structure. An angle of 75° was chosen because it is steeper than normally being built, but no so steep that crushing is expected.

The is no accepted method for the production of ice ridges in model-scale; it applies both to the theoretical foundation and the practical procedures (Repetto-Llamazares, 2010). Complete thermo-mechanical testing is practically almost impossible (Høyland, 2010), and compromises must be made. In the project, we will investigate how the initial conditions and the consolidation after ridge production govern the thickness of the consolidated layer and the mechanical properties of the rubble and the consolidated layer.

2. Scaling

We assume that gravity and water and ice densities are similar in full-scale (prototype) and basin-scale (model). Further, inertia, gravity/buoyancy, ice strength, and ice elasticity may govern the process. One may attempt to scale the forces and/or the deformation patterns. In the latter case, the ice's elastic behavior is vital, but the elastic contribution to the total ice load on a rigid structure is probably not vital. When considering the full dynamic ice-structure interaction, the elasticity may be important. Let us concentrate on the scaling of the ice load, identify force contributions from inertia, gravity/buoyancy, and ice breaking (strength) so that the total force F can be expressed:

$$F = f\left(F_{in}, F_g, F_{is}\right) \qquad\qquad \textbf{[1]}$$

where F_{in} is the inertia, F_g is the gravity/buoyancy, and F_{is} is the ice strength contribution. And they scale as follows:

$$F_{in} \sim \frac{v^2}{L} \qquad\qquad F_g \sim L^3 \qquad\qquad F_{is} \sim \sigma L^2 \qquad\qquad \textbf{[2]}$$

where v is a vital velocity, L a vital length, and σ an ice strength. From these, we may identify two dimensionless ratios, the Froude number Fr and an *Ice strength* or *Strength of Materials number SOM*:

$$Fr = \frac{v^2}{gL} \qquad\qquad SOM = \frac{v^2}{\sigma} \qquad\qquad \textbf{[3]}$$

Note that the Cauchy number does not directly come into play unless $\left(\dfrac{\sigma}{E}\right)_p = \left(\dfrac{\sigma}{E}\right)_m$ which is

challenging to obtain.

In our case, we tested both a conical and a vertical structure shape so that we should consider both ice ride-up and bending failure as well as crushing. If ride-up (or down) and bending failure is vital, we assume F_{in}, F_g, and F_{is} are all vital, and further that ice strength is dominated by flexural strength (σ_f). It is then well known that the geometric, kinetic, strength, and dynamic scaling factors become:

$$\lambda = \frac{h_{i,p}}{h_{i,m}} = \frac{w_p}{h_m} \qquad\qquad \lambda_k = \sqrt{\lambda} \qquad\qquad \lambda_\sigma = \lambda \qquad\qquad \lambda_d = \lambda^3 \qquad\qquad \textbf{[4]}$$

where h_i is the ice thickness, w the structure width, and the indices p and m refer to respectively prototype (full-scale) and model (basin-scale).

In the case of crushing, one may imagine that gravity/ buoyancy does not play a vital role so that the total force can be expressed:

$$F = f\left(F_{in}, F_{is}\right) \qquad\qquad \textbf{[5]}$$

where the ice breaking is dominated by crushing and expressed through a compressive strength (σ_{cr}). Now the Froude number is irrelevant, and only the strength number governs the process so that there are no conditions on how to determine the ice strength (except that it should be proportional to velocity squared). The ice force is a function of length squared and the ice strength, and one may use any ice strength! In our case, we tested the two structure shapes with the same ice, and we had the ridge keels, so it is evident that we need to consider gravity/buoyancy contributions and use Fr so that the ice should be weakened ($\lambda_\sigma = \lambda$).

The next question that may come up is, what is the ice strength? How can one carry out a test in full-scale and basin-scale and compare them? When ice fails in bending, the flexural strength is used, and it is tested (more or less) the same way in full-scale and basin-scale. The full ice thickness is tested, and flexural strength is derived, often based on linear elastic beam theory, so that it is a force with units of stress. The ice compressive strength is more complicated, it is not a well-defined property, and in the field, there are three tests: a) Uni-axial compressive strength, with often cylindrical samples of diameter/length of

70mm/175mm; b) Borehole-Jack indentation tests, where the piston head is roughly 50mm; and c) a few compressive tests of full ice thickness have been done, but only for relatively thin ice or low loading-rate. Testing full ice thickness (e.g.1m) compressive strength in the field requires very large and heavy equipment and is practically difficult to carry out. In a basin, the compressive strength is tested either by a) Making short beams (width and length approximately equal) and compressing full thickness or b) Making indentation with a small cylinder into a strait ice edge. In other words, the compressive strength is not a well-defined property, and different tests are done in the field and in model-scale. A comparison between full-scale and model-scale is difficult. We also need thermal scaling as the consolidated layer is the result of thermal processes; the state-of-the-art, including challenges, are given in Høyland (2007), Høyland (2010), and Repetto-Llamazares (2010) and will not be repeated here.

3. Experimental set-up and procedures

### 3.1 Level ice and ridge production

The water in the Aalto basin is doped with ethanol, resulting in a concentration of ethanol 0.3%. The level ice was created in the standard, for this basin, procedure by spraying and letting the ice grow upwards. The air temperature during spraying was -10C, while the ice was isothermal at the freezing point. When the target ice thickness of 40 mm was reached, the spraying stopped, but the cooling continued to cool the ice and create a proper internal ice matrix and strength. Finally, the ice was tempered to achieve target strength. The ridges were produced in two steps. Firstly, by breaking the ice with the pushing plates on the main carriage, and secondly, by pushing it together with the carriage. When the ridge was formed, it had to be kept in place by a confining level ice floe (Figure 1). The campaign resulted in ten tests, varying shape of the structure, ridge consolidation degree, and level ice properties (Table 1). If the testing matrix required the run through the unconsolidated keel (Tests 2, 7, and 8), the experiment was conducted at once after ridge production. Otherwise (Tests 1, 5, 6, 9, and 10), cooling was applied overnight to run the ridge consolidation process; it followed by warming to maintain target level ice strength properties. During the test campaign, three cycles of ice level sheet production followed by ice ridge creation and consolidation were carried out; air temperature courses during these cycles were registered with regular basin sensor and thermistor string placed in the ice (Figure 2). Moments of structure-ice interaction tests and level ice strength tests are indicated on the temperature course plots.

Table 1. Testing matrix with varied structure shape, keel consolidation, and ice properties. Note that Tests 3 and 4 failed and their results are not used further in the discussion.

Ice sheet	Test #	Structure waterline	Structure Interactions with			Level ice flexural strength (MPa)
			Level ice before	Ridge	Level ice after	
1	1	Vertical	No	consolidated	No	73
2	2	Vertical	Yes	unconsolidated	Yes	60
	5	Sloping	No	consolidated	Yes	235
	6	Sloping	Yes	consolidated	Yes	-
3	7	Sloping	Yes	unconsolidated	Yes	51
	8	Sloping	Yes	unconsolidated	Yes	-
	9	Sloping	Yes	consolidated	Yes	78
	10	Vertical	No	consolidated	No	-
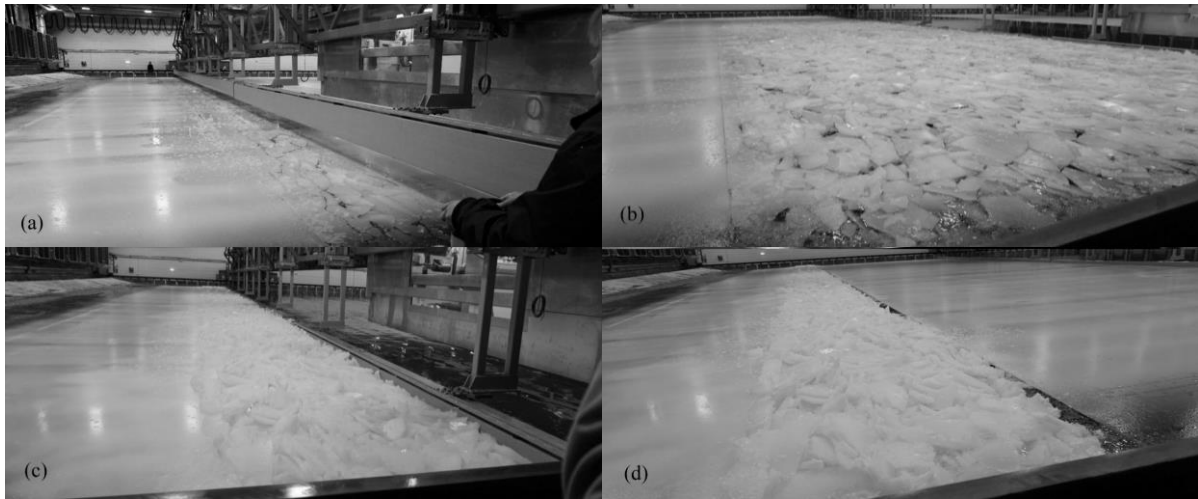
Figure 1. Ridge production. Cutting level ice (a), cutting completed (b), forming the ridge by pushing broken level ice (c), ridge production completed (d).
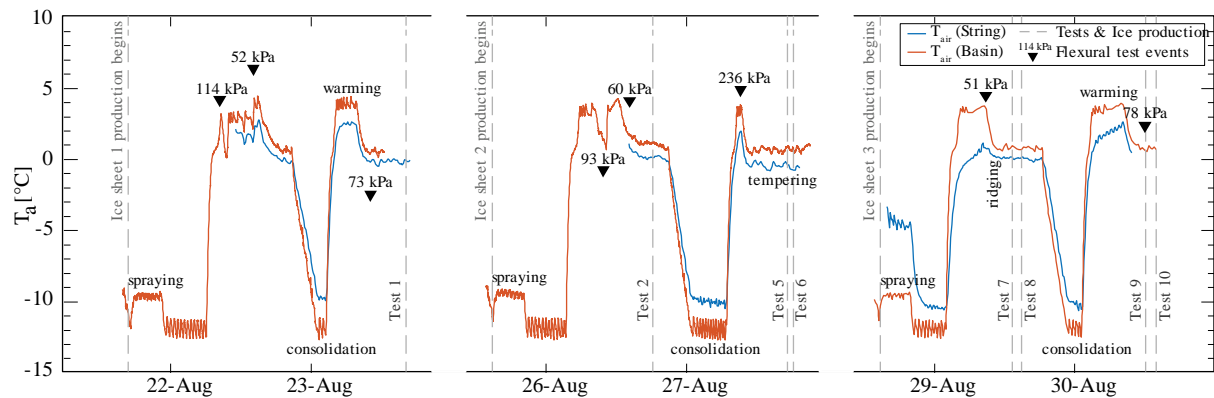
Figure 2. The air temperature history measured by the Aalto sensor and one of the thermistor strings.

3.2 Mechanical characterization level ice and ridges

Mechanical parameters were tested for both level ice and the ice ridges. For level ice, flexural and compressive strengths were measured, and for the ridges, punch tests were carried out using regular Aalto ice basin tests' procedures. The flexural strength was tested on cantilever beams 25 cm long and 8 cm wide (Figure 3). The compressive strength was tested by compressing short cantilever beams.

Figure 3. Testing level ice flexural strength

3.3 Structure, loads, and cameras

The structure with vertical and sloping walls was tested (Figure 4). The structure's position was adjusted for different scenarios: cylindrical shape at the waterline and conical shape at the waterline. The structure was assumed to be rigid, even though, in reality, neither the fixing of the structure to the wagon nor the wagon itself were completely rigid. We did not measure any structural response. The cylindrical structure diameter was 54.2 cm, and this was also the cone bottom's diameter on the conical structure. The cone angle was 74.8° and the cone height was 35.8 cm. The global load was measured with a three-dimensional load cell between the carriage and the structure. Also, local pressure distribution was registered with tactile sensors installed both at the cylindrical and conical structures. However, due to damage to the tactile sensors in the tests, data were only gathered from tests 1, 2, and 3. A system of cameras below and above water surface was installed. Cameras below water were intended to provide the view and depth measurement of rubble pile accumulation in front of the structure and the side view of the rubble pile passing the structure. The camera in the air was set to provide the top view covering structure-ice interaction and the zone ahead of that, such that if there is visible crack propagation, it was registered. GoPro cameras powered by power banks were packed in waterproof cases, which were mounted on a steel frame with long arms. The frame itself was mounted on the carrier behind the structure to avoid causing any interaction with ice or disturbances into load measurements. In turn, long arms below the structure were reaching out to provide the requested view of the process. Power banks kept cameras recording throughout the working day. This allowed us to mount and dismount the camera's frame only once per day, which helped for the tests program's efficiency.
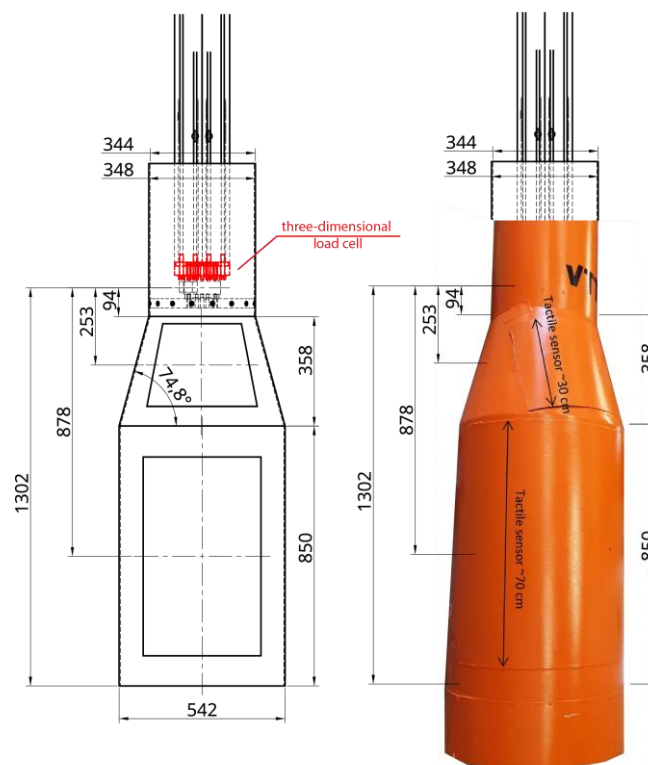

Figure 4. Front view cross-section sketch and photo of the structure used in the experiment. Dimensions and location of three-dimensional load cell and tactile sensors on the structure's vertical and sloping wall.

## 4. Some observations and preliminary results

4.1 Level ice and ridge - geometry and morphology

Three ice sheets were produced, and three ice ridges were built, resulting in ten structure test runs (Table 1). Some transverse profiles (cross-sections) of the ridge made in ice sheet three are shown in Figure 5. The maximum depth of keel was approximate 0.4 m. The width of the ridge was generally 4 m and started from the side close to the structure. One can see that the keel profile was roughly in the shape of a trapezoid, which is similar to the geometry of a natural ridge keel.
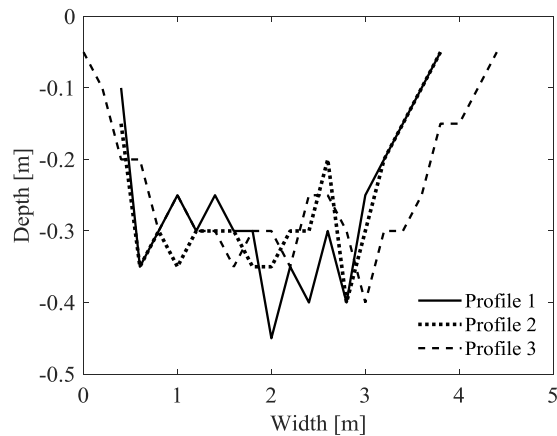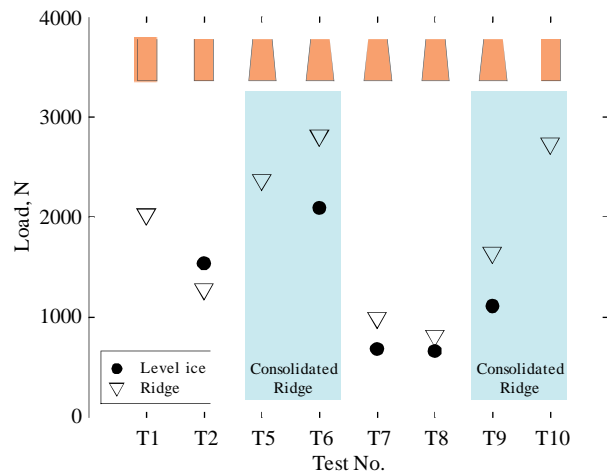

Figure 5. Cross-section profiles of the ridge made from ice sheet number three.

4.2 Ice forces
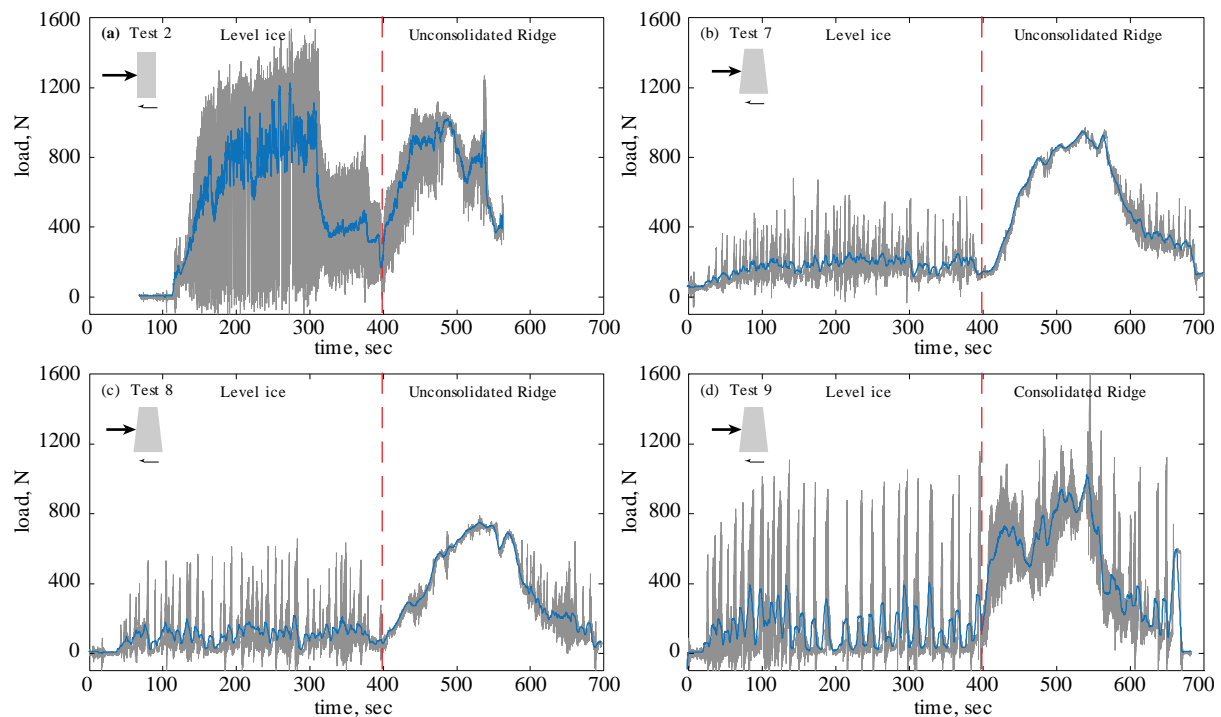
Figure 6. Horizontal ice load in the towing direction. In grey − raw signal, in blue − smoothed signal. a) Test 2, vertical structure, unconsolidated; b) Test 7, sloping structure, unconsolidated; c) Test 8, sloping structure, unconsolidated; d) Test 9, sloping structure, consolidated.

**Figure 7.** Peak loads from level ice and ridges in all tests.

The loads from level ice and ridges are given as time-series (Figure 6) and as peak loads (Figure 7). Let us compare loads of a) vertical and sloping structures, b) consolidated and unconsolidated ridges, and c) level ice and ridges.

The load on the vertical structure was generally higher than on the sloping structure (Tests 1, 2 versus Tests 7, 8; and Test 10 versus Test 9), and the load from consolidated ridges was higher than from unconsolidated ridges. Both these observations are as expected. The findings from the comparison of level ice and ridge loads are more interesting. For the vertical structure, the load from level ice was higher than from the ridge (Test 2), whereas it was the opposite of the sloping structure.

The difference between the raw signal and the smoothed signal (Figure 6) indicates significant dynamic amplification, but a proper dynamic analysis is outside the paper's scope and motivation. We neither measured the structural accelerations nor its dynamic properties. Figures 8 and 9 show the frequency domain of the load-time series for the level ice and ridge and allows for some observations. All the loads on the sloping structure contained a low-frequency component that could not be seen in the vertical structure's signals. This corresponds to the visual observations of ice ridging-up on and releasing from the cone. Further, it seems to be a difference between consolidated (Test 9) and unconsolidated (Tests 7 and 8) ridge action on the cone (Figure 9). In the consolidated ridge, the low-frequency component was smaller, indicating that the cone was less effective in avoiding crushing.

The differences between ice actions on vertical and conical structures for level ice and ridges indicate that the cone is less effective in reducing loads from ridges, and especially consolidated ridges, than from level ice. In level ice, the pile-up height mostly did not exceed the cone, while in ridge interaction, it often did. This argues that the ISO approach to treating the consolidated layer as thick level ice is questionable. Earlier observations from HSVA (Jensen et al., 2001) confirm that the ridge load on a ship-shaped vessel (sloping) was higher than from level ice.
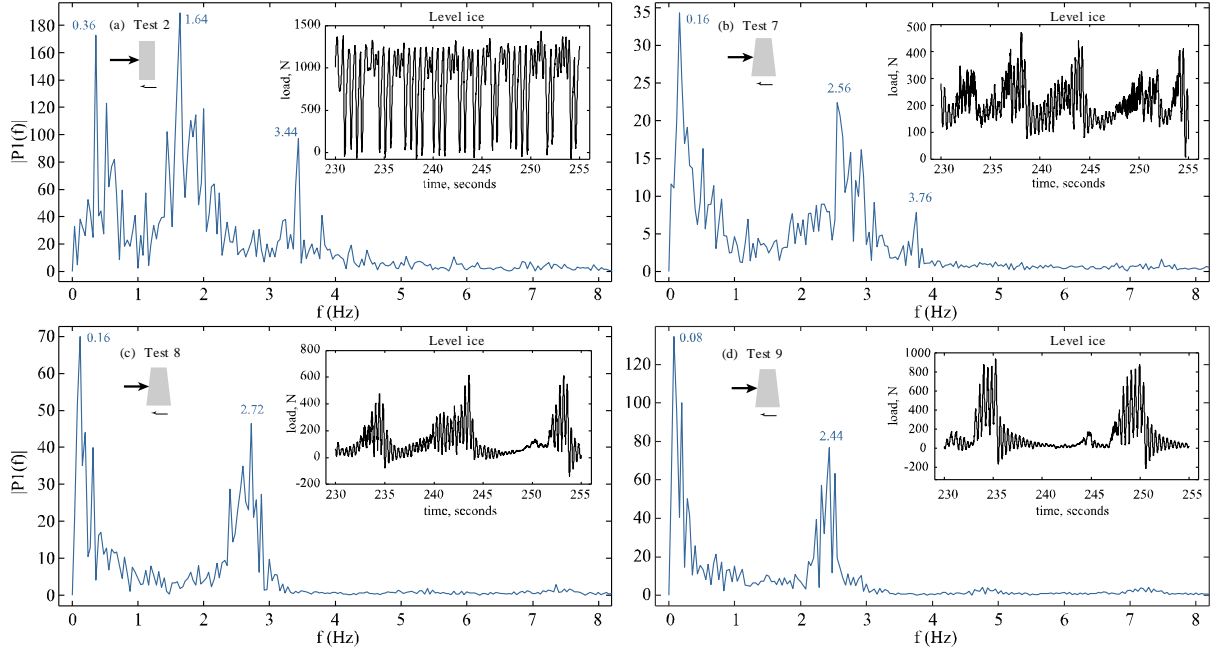
Figure 8. Frequency domain analysis of horizontal load signal during structure advancing through level ice. Note, the vertical scale is different both for load signal and FFT analysis.
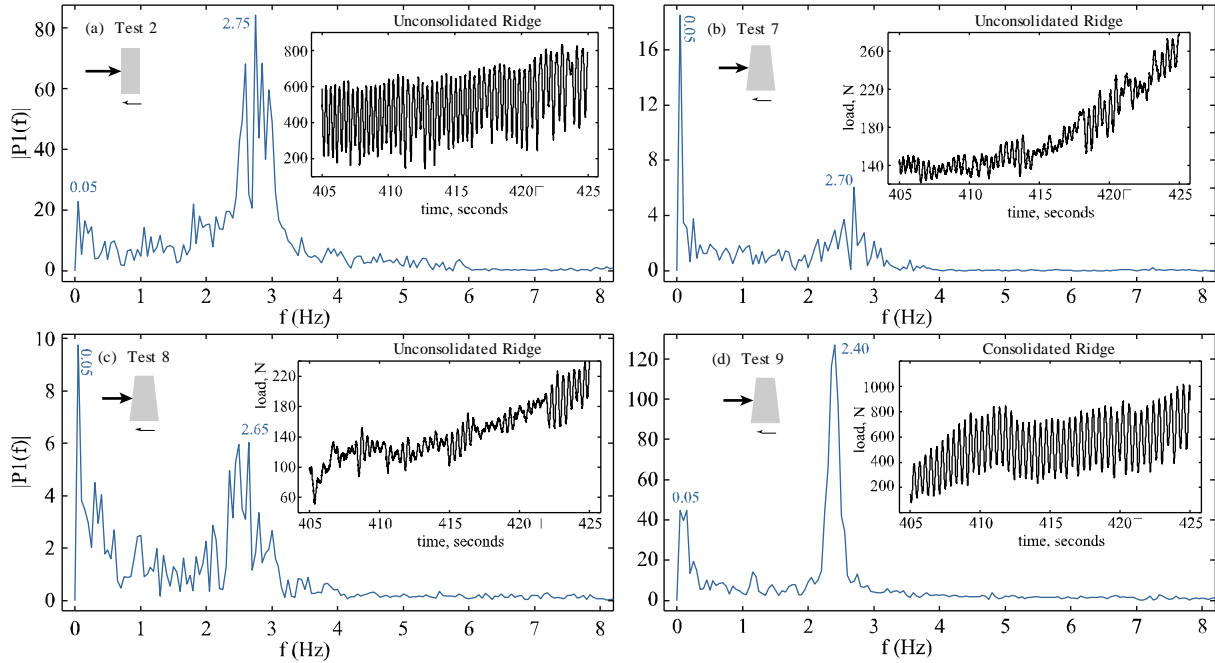
Figure 9. Frequency domain analysis of horizontal load signal during structure advancing through the ridge. Note, the vertical scale is different both for load signal and FFT analysis.

The main preliminary observations are that horizontal load from level ice on vertical structure (F^V_{li}) gave the highest level; the load from a ridge on vertical structure (F^V_{ri}) was higher than load from the ridge on sloping structure (F^S_{ri}); and, finally, the load from level ice on sloping structure gave the lowest level (Equation 6).

$$F^V_{li} > F^V_{ri} > F^S_{ri} > F^S_{li}$$ [6]

5. Conclusions

A set of experiments were carried out in the Aalto ice basin to investigate the scaling of first-year ridges and the effect of cone angle on the ridge load on fixed structures. The ridges were produced by breaking the level ice and pushing the broken pieces together. The ridges were 40 m long, about 4 m wide, and approximately 0.4 m deep. After formation, half of the ridge was tested mechanically, and ridge-structure interaction testing was done. Then the ridge consolidated overnight, and the procedure of testing mechanical properties and interaction with structures repeated the next day. The load analysis's main preliminary results are that horizontal load from level ice on vertical structure (F^V_{li}) gave the highest level. Next, in decreasing order of magnitude, followed the loads from a ridge on vertical structure (F^V_{ri}), from a ridge on sloping structure (F^S_{ri}), and finally, from level ice on sloping structure (F^S_{li}).

References

Dolgopolov, Y., Afanasiev, V.P., Koren'Kov, V.A. and Panfilov, D.F., 1975. Effect of hummocked ice on the piers of marine hydraulic structures. International Symposium on Ice Problems, 3rd, Proceedings, Dartmouth College, Hanover, NH. Aug., 18-21. 1975.: 469-477.

Høyland, K.V., 2007. Thermal scaling of ice ridges, some dimensionless numbers. Proceedings of the 19th International Conference on Port and Ocean Engineering under Arctic Conditions (POAC), Dalian, China. pp. 517-523, ISBN 978-7-5611-3631-7.

Høyland, K.V., 2010. Thermal aspects of model basin ridges. Proceedings of the 20th IAHR International Symposium on Ice, June 14 to 18, Lahti, Finland, paper 66.

ISO19906, 2019. Petroleum and natural gas industries - Arctic offshore structures, Geneva, Switzerland, pp. 434.

Jensen, A., Løset, S., Høyland, K.V., Liferov, P., Heinonen, J., Evers, K.-U. and Maattanen, M., 2001. Physical modelling of first-year ice ridges - part II: mechanical properties. Proceedings of the 16th International Conference on Port and Ocean Engineering under Arctic Conditions, POAC'01, 3: 1493-1502.

Repetto-Llamazares, A.H.V., 2010. Review in model basin ridges. Proceedings of the 20th IAHR International Symposium on Ice, June 14 to 18, Lahti, Finland, paper 154.

Serré, N. and Liferov, P., 2010. Loads from ice ridge keels – experimental vs. numerical vs analytical. Proceedings of the 20th IAHR International Symposium on Ice, June 14 to 18, Lahti, Finland, paper 92.